Monthly Notices
of the
ROYAL ASTRONOMICAL SOCIETY

Mon. Not. R. Astron. Soc. **419,** 3608–3623 (2012) doi:10.1111/j.1365-2966.2011.20010.x

UBVI CCD photometry and star counts in nine inner disc Galactic star clusters★

Giovanni Carraro[1]†‡ and Anton F. Seleznev[2]†§

[1]*European Southern Observatory, Alonso de Cordova 3107, Casilla 19001, Santiago 19, Chile*
[2]*Astronomical Observatory, Ural State University, Lenin Avenue 51, Ekaterinburg 620083, Russia*

Accepted 2011 October 13. Received 2011 October 13; in original form 2011 August 31

ABSTRACT

We present and discuss new CCD-based photometric material in the *UBVI* passbands for nine Galactic star clusters located inside the solar ring, for which no CCD data are currently available. These star clusters are IC 2714, NGC 4052, ESO 131SC09, NGC 5284, NGC 5316, NGC 5715, VdB-Hagen 164, NGC 6268 and Czernik 38. The main aim of this study is to establish the nature of real clusters or random field star enhancements and, when real, estimate their fundamental parameters. To this aim, we first perform star counts by combining our optical photometry with 2MASS, and derive cluster sizes and radial density profiles. The fundamental parameters such as age, reddening and distance are then inferred from the analysis of the star distribution in the colour–colour and colour–magnitude diagrams of only the spatially selected likely members. Our analysis shows that ESO 131SC09, NGC 5284 and VdB-Hagen 164 are most probably not clusters, but random enhancements of a few bright stars along the line of sight, with properties much similar to so-called open cluster remnants. The remaining clusters are physical groups and are all younger than about 1 Gyr. We use the newly derived set of parameters, in particular distance and reddening, to investigate their position in the Galaxy in the context of the spiral structure of the Milky Way. We find that the youngest clusters (IC 2714, NGC 5316 and NGC 6268) are located close to or inside the Carina–Sagittarius arm, and are therefore bona fide spiral structure tracers. On the other hand, the oldest clusters (Czernik 38, NGC 4052 and NGC 5715) are floating in the interarm space between the Carina–Sagittarius and the more distant Scutum–Crux arm. Interestingly enough, the oldest clusters of this sample – Czernik 38 and NGC 5715 – are among the few known open clusters to be older or as old as the Hyades in the inner Galactic disc, where star clusters are not expected to survive for a long time, because of the strong tidal field and the higher probability of close encounters.

Key words: Galaxy: disc – open clusters and associations: general – open clusters and associations: individual: – galaxies: photometry – galaxies: spiral.

1 INTRODUCTION

In the Milky Way (MW), stellar clusters form in dense regions located inside spiral arms. When clusters survive, they remain connected with the parent arm for about 100 Myr (Dobbs & Pringle 2010). Afterwards, they decouple from it and are no longer useful as spiral structure tracers. Young star clusters have been used for half a century to probe the spiral structure of the MW. Historically, the first arms to be detected using young open clusters were the Perseus arm in the second Galactic quadrant, the Carina–Sagittarius in the fourth quadrant and the Orion spur in which the Sun is embedded (Trumpler 1930). Today, the picture we have of the MW spiral structure contains many more details (Russeil 2003; Efremov 2011; Lépine et al. 2011), although a lively discussion is still ongoing as to how many major arms are present and if they are long-lived or transient (Grosbol, Carraro & Beletski 2011).

In the last decade, young star clusters played a major role in improving our knowledge of the MW spiral structure, especially in the third Galactic quadrant. Moitinho et al. (2006), Vázquez et al. (2008) and Carraro et al. (2010) identified for the first time in optical observations the outer Norma–Cygnus arm and clarified the

★Based on observations collected at the Cerro Tololo Inter-American Observatory and Las Campanas Observatory, Chile.

†E-mail: gcarraro@eso.org (GC); anton.seleznev@usu.ru (AFS)
‡On leave from Dipartimento di Astronomia, Universitá di Padova, Italy.
§ESO Visiting Scientist.

© 2011 The Authors
Monthly Notices of the Royal Astronomical Society © 2011 RAS

Downloaded from http://mnras.oxfordjournals.org/ at Ural Federal University on March 27, 2015

Table 1. Basic parameters of the clusters under investigation. Coordinates are for J2000.0. In the last two columns we report the extinction at infinity and the observatory where data were taken.

Number	Name	RA	Dec.	l	b	$E(B-V)$	Observatory
		($^{\rm h}$ $^{\rm m}$ $^{\rm s}$)	($^\circ$ $'$ $''$)	($^\circ$)	($^\circ$)	(mag)	
1	IC 2714	11:17:27.0	−62:44:00.0	292.40	−1.799	2.77	LCO
2	NGC 4052	12:01:12.0	−63:13:12.0	297.30	−0.900	4.15	LCO
3	ESO 131SC09	12:29:37.4	−57:52:31.0	300.02	4.873	0.87	CTIO
4	NGC 5284	13:46:29.9	−59:08:39.0	309.95	2.975	1.25	CTIO
5	NGC 5316	13:53:57.0	−61:52:06.0	310.23	0.115	12.02	LCO
6	NGC 5715	14:43:29.0	−57:34:36.0	317.53	2.085	1.78	LCO
7	VdB-Hagen 164	14:48:13.7	−66:20:12.0	314.28	−6.070	0.32	CTIO
8	NGC 6268	17:02:00.8	−39:44:18.0	346.10	1.216	5.81	CTIO
9	Czernik 38	18:49:42.0	+05:52:00.0	37.13	2.630	2.08	CTIO

shape and interaction of the Orion and Perseus arms. These studies made it clear that young star clusters are powerful spiral tracers when it is possible to determine their distance and age with high confidence. In particular, the authors stress how crucial the deep *U*-band photometry is to pin down cluster reddening and hence obtain their distance.

We also present and discuss the *UBVI* photometry of nine star clusters, all located in the fourth Galactic quadrant except for one, Czernik 38, which is located in the first quadrant (see Table 1). According to most public catalogues, most of the star clusters are nothing but simple star cluster candidates and lack published data. However, we expect that they are mostly young clusters based on both an inspection of DSS maps and the well-known idea that clusters cannot survive for long in the inner Galactic disc.

Apart from the obvious goal of establishing their nature and deriving their fundamental parameters, we aim to use them – when they are sufficiently young – as spiral arm tracers in the longitude range $290^\circ \leq l \leq 360^\circ$. In this MW sector, inside the solar ring, we expect the lines of sight of the clusters to first encounter the Carina–Sagittarius arm, and hopefully, also the Scutum–Crux arm, which is much closer to the Galactic Centre, as well as the Perseus arm, which is much further away (Vázquez et al. 2005; Baume, Carraro & Momany 2009; Carraro & Costa 2009).

The technique we used is based on the analysis of the colour–colour and colour–magnitude diagrams of groups of stars properly selected after having performed star counts and defined clusters' reality and size (see Seleznev et al. 2010 for details).

As a consequence, this paper is organized as follows. In Section 2, we present information culled from the literature on the objects under investigation, which demonstrate that they have almost completely been overlooked in the past. Section 3 presents the observations and basic data reduction, together with photometric calibration, completeness analysis and cross-correlation with 2MASS. The comparison with previous photometry – when available – is discussed in Section 4. Section 5 is devoted to star counts and the derivation of clusters' size. We then estimate the method to infer clusters' fundamental parameters in Section 6. Section 7, finally, discusses the outcome of this analysis. The conclusions of this investigation, together with suggestions/recommendations for further studies, are provided in Section 8.

2 PREVIOUS INVESTIGATIONS

Most clusters in the sample we investigated for this paper have not been studied earlier, and only for Czernik 38, some preliminary CCD data have been provided.

We present here a cluster-by-cluster compilation of previous studies from the literature to date.

IC 2714. This is the star cluster of the whole sample which received more attention in the past. We selected this cluster also as a control object for our photometry, which we compare in Section 4.

The *UBV* photoelectric photometry of about 200 stars has been presented by Claria et al. (1994), together with spectroscopy of 14 probable giant star members of the cluster. These authors derived an age of 300 Myr and place the cluster at a distance of 1300 pc, in agreement with findings of Becker (1960). They found that the cluster suffers from variable extinction, and obtain $E(B-V) = 0.36$ and 0.37 from the turn-off and giant stars, respectively. As for the metallicity, they found a large range of values, from +0.05 using David Dunlap Observatory (DDO) to −0.18 using the Whasington photometric system. A revision of the DDO calibration led Twarog, Ashman & Anthony-Twarog (1997) to provide [Fe/H] ranging from −0.01 to 0.02, and $E(B-V) = 0.35$. More recently, spectroscopic analysis by Santos et al. (2009) confirmed the range of metallicity found by Twarog et al. (1997), ruling out the results of the Washington photometry. Finally, Smiljanic et al. (2009) derived [Fe/H] = 0.12 as well as reddening $E(B-V) = 0.33$ from one giant. By adopting Shaller et al. (1992) isochrones, they fitted Claria et al. (1994) photometry, obtaining an apparent distance modulus of $(m-M) = 11.5$ and an age of 400 Myr.

NGC 4052. van den Berg & Hagen (1975) describe NGC 4052 of a medium richness, real cluster, mostly composed of blue stars, and possibly embedded in some nebulosity. The shallow study of Kharchenko et al. (2005) provides preliminary estimates of the cluster parameters based on photometry and astrometry of fewer than 20 stars brighter than $V \sim 12$. They locate this 250-Myr-old cluster at 1200 pc from the Sun. No CCD studies of NGC 4052 have been conducted so far.

ESO 131SC09. No information is available for this cluster apart from its size, which is around 5 arcmin according to Dias et al. (2002).

NGC 5284. No information is available for this cluster beyond its mere classification.

NGC 5316. The only available study for this cluster is the photoelectric investigation by Ramin (1966) down to $V \sim 16$, which places the cluster at a heliocentric distance of 1200 pc. The age of 150 Myr is derived by Kharchenko et al. (2005) from a subsample of stars brighter than $V \sim 12$. Its young age is also recognized by the visual inspection of van den Berg & Hagen (1975).

NGC 5715. van den Berg & Hagen (1975) describe NGC 5715 of a medium richness, real cluster, mostly composed of blue stars. No optical study is available for NGC 5715; however, its properties

Downloaded from http://mnras.oxfordjournals.org/ at Ural Federal University on March 27, 2015

have been investigated using 2MASS by Bonatto & Bica (2007). They report an age of 800 Myr and a distance of 1.5 kpc from the Sun.

Vdb-Hagen 164. van den Berg & Hagen (1975) describe this cluster as a very poor ensemble of blue stars. No data are available for it to date.

NGC 6268. Seggewiss (1968) provided some photographic photometry of NGC 6268 down to $V \sim 14$, and its analysis led to a heliocentric distance of 1200 pc. Later, van den Berg & Hagen (1975) described it as a very poor ensemble of blue stars. The shallower study by Kharchenko et al. (2005) found a somewhat smaller distance of 1000 pc, and suggests an age around 15 Myr, lending support to van den Berg & Hagen's (1975) visual impressions.

Czernik 38. Discovered by Czernik (1966), this cluster is described as a relatively rich cluster with a diameter of 14 arcmin. Schmidt camera CCD photometry has recently been obtained by Maciejewski (2008), which suggests that the cluster is at least 1-Gyr old and at a heliocentric distance of 1200 pc.

3 OBSERVATIONS

In this section, we provide details of how we conducted observations and reduced the collected data. Five of the programme clusters (ESO 131SC09, NGC 5284, VdB-Hagen 164, NGC 6268 and Czernik 38) were surveyed at the Cerro Tololo Inter-American Observatory[1] (CTIO), while the remaining four clusters (IC 2714, NGC 4052, NGC 5316 and NGC 5715) were imaged at the Las Campanas Observatory[2] (LCO). Their equatorial and Galactic coordinates for the 2000.0 equinox are reported in Table 1, together with an estimate of the reddening from FIRB (Schlegel et al. 1998). The last column indicates where each cluster was observed. Fig. 1, finally, shows DSS images of the nine fields where the clusters are located.

Because of the differences in both telescopes and detectors, we separately describe the observations and data reduction of the two cluster groups.

3.1 CTIO observations

These regions were observed with the Y4KCAM camera attached to the CTIO 1-m telescope, operated by the SMARTS consortium.[3] This camera is equipped with an STA 4064 × 4064 CCD[4] with 15-μm pixels, yielding a scale of 0.289 arcsec pixel^{-1} and a field of view (FOV) of 20 × 20 arcmin^2 at the Cassegrain focus of the CTIO 1-m telescope. The CCD was operated without binning, at a nominal gain of 1.44e$^-$ ADU^{-1}, implying a readout noise of 7e$^-$ per quadrant (this detector is read by means of four different amplifiers).

In Table 2 we present the log of our *UBVI* observations. All observations were carried out in photometric, good-seeing (always less than 1.2 arcsec) conditions. Our *UBVI* instrumental photometric system was defined by the use of a standard broadband Kitt Peak $UBVI_{kc}$ set of filters.[5] To determine the transformation from our instrumental system to the standard Johnson–Kron–Cousins system and to correct for extinction, we observed stars in Landolt's areas PG 1047, PG 1323, G26 and MarkA (Landolt 1992) multiple times and with airmasses ranging from ∼1.03 to ∼2.0, and covering a large colour range $-0.3 \leq (B - V) \leq 2.0$ mag.

3.2 LCO observations

Four clusters were observed at LCO (see Table 1) on the nights of 2010 May 8–10, as illustrated in Table 3. The clusters were observed using the SITe#3 CCD detector onboard the Swope 1.0-m telescope. With a pixel scale of 0.435 arcsec pixel^{-1}, this CCD allows us to cover 14.8 × 22.8 arcmin on the sky. To determine the transformation from our instrumental system to the standard Johnson–Kron–Cousins system and to correct for extinction, we observed stars in Landolt's areas PG 1047, PG 1323, PG 1633, PG 1657 and MarkA (Landolt 1992) multiple times and with airmasses ranging from ∼1.05 to ∼1.9, and covering a large colour range $-0.4 \leq (B - V) \leq 2.1$ mag (see Table 3). We secured night-dependent calibrations.

3.3 Photometric reductions

The basic calibration of the CCD frames was carried out using IRAF[6] package CCDRED. For this purpose, zero-exposure frames and twilight sky flats were taken every night. Photometry was then performed using the IRAF, DAOPHOT/ALLSTAR and PHOTCAL packages. Instrumental magnitudes were extracted following the point-spread function (PSF) method (Stetson 1987). A quadratic, spatially variable, master PSF (PENNY function) was adopted, because of the large FOV of the two detectors. Aperture corrections were then determined making aperture photometry of a suitable number (typically 10–20) of bright, isolated, stars in the field. These corrections were found to vary from 0.160 to 0.290 mag, depending on the filter. The PSF photometry was finally aperture corrected, filter by filter.

3.4 Photometric calibration

After removing problematic stars, and stars having only a few observations in the Landolt (1992) catalogue, our photometric solution for the CTIO run, extracted from a total of 92 measurements per filter, turned out to be

$$\begin{aligned}
U &= u + (3.110 \pm 0.010) + (0.45 \pm 0.01) \\
&\quad \times X - (0.010 \pm 0.006) \times (U - B), \\
B &= b + (2.143 \pm 0.012) + (0.27 \pm 0.01) \\
&\quad \times X - (0.118 \pm 0.007) \times (B - V), \\
V &= v + (1.740 \pm 0.007) + (0.15 \pm 0.01) \\
&\quad \times X + (0.038 \pm 0.007) \times (B - V), \\
I &= i + (2.711 \pm 0.011) + (0.08 \pm 0.01) \\
&\quad \times X + (0.041 \pm 0.008) \times (V - I).
\end{aligned}$$

The final rms of the fitting was 0.030, 0.015, 0.010 and 0.010 in U, B, V and I, respectively.

[1] Available from http://www.ctio.noao.edu
[2] Available from http://www.lco.cl
[3] Available from http://http://www.astro.yale.edu/smarts
[4] Available from http://www.astronomy.ohio-state.edu/Y4KCam/detector.html
[5] Available from http://www.astronomy.ohio-state.edu/Y4KCam/filters.html

[6] IRAF is distributed by the National Optical Astronomy Observatory, which is operated by the Association of Universities for Research in Astronomy, Inc., under cooperative agreement with the National Science Foundation.

Downloaded from http://mnras.oxfordjournals.org/ at Ural Federal University on March 27, 2015

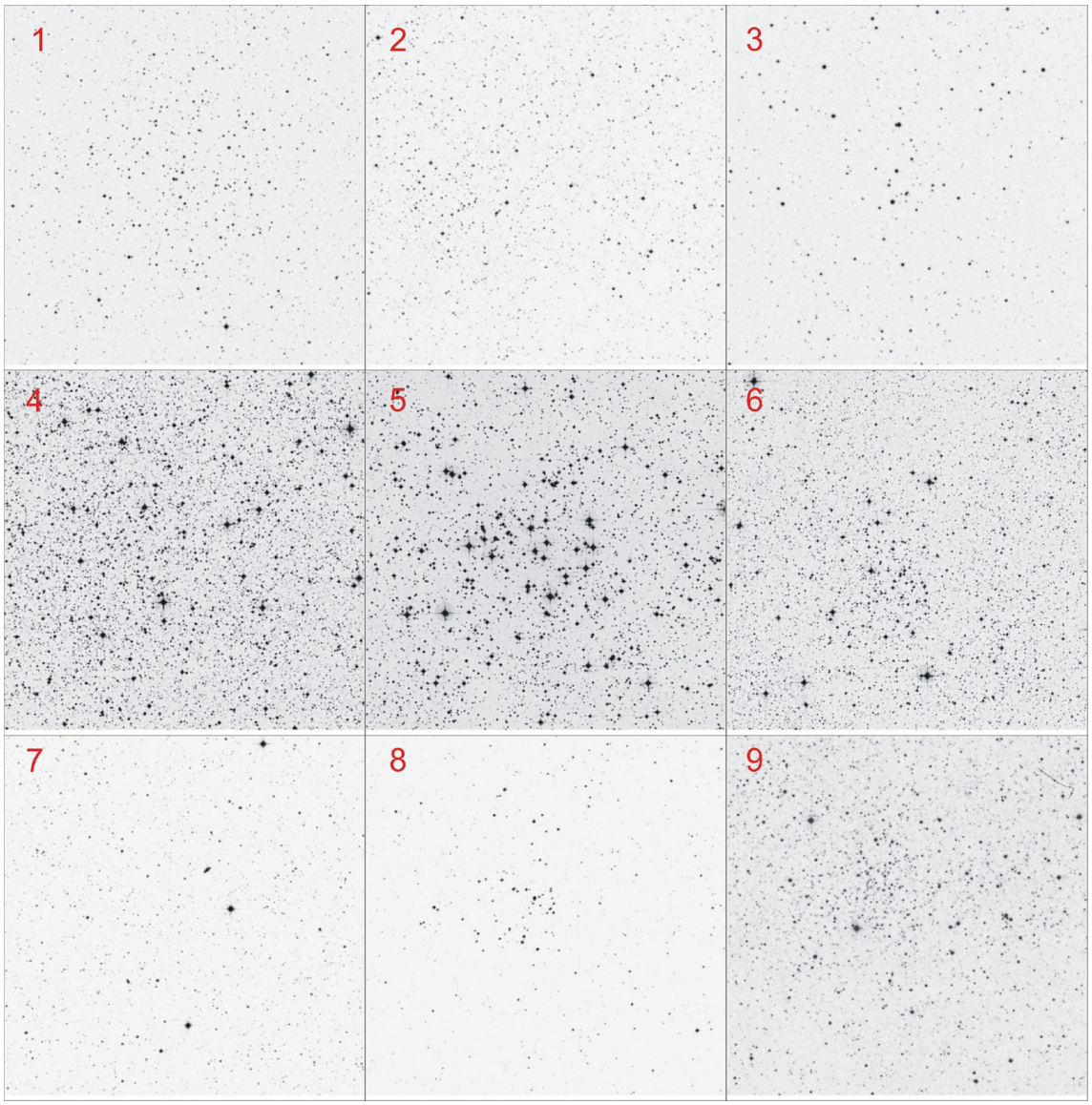

Figure 1. DSS images centred on the nine programme clusters. North is up, east to the left and the FOV is 20 arcmin on a side. Images follow the numbering as given in Table 1 from top left to bottom right.

As for LCO observations, we provided individual night-based photometric solutions. However, since the three solutions were identical, we merged and averaged them together in a single photometric solution. This implies a total of 103 measures per filter and the solutions read:

$$U = u + (4.902 \pm 0.010) + (0.41 \pm 0.01) \times X + (0.129 \pm 0.020) \times (U - B),$$

$$B = b + (3.186 \pm 0.012) + (0.31 \pm 0.01) \times X + (0.057 \pm 0.008) \times (B - V),$$

$$V = v + (3.115 \pm 0.007) + (0.17 \pm 0.01) \times X - (0.057 \pm 0.011) \times (B - V),$$

$$I = i + (3.426 \pm 0.011) + (0.07 \pm 0.01) \times X + (0.091 \pm 0.012) \times (V - I).$$

The final rms of the fitting in this case was 0.040, 0.025, 0.015 and 0.015 in U, B, V and I, respectively.

Global photometric errors were estimated using the scheme developed by Patat & Carraro (2001, appendix A1), which takes into account errors resulting from the PSF fitting procedure (i.e. from ALLSTAR/ALLFRAME), and the calibration errors (corresponding to the zero-point, colour terms and extinction errors). In Fig. 2, we present our global photometric errors in V, $(B - V)$, $(U - B)$ and $(V - I)$ plotted as a function of the V magnitude. A quick inspection shows that stars brighter than $V \approx 20$ mag have errors lower than $\sim$0.05 mag and lower than $\sim$0.10 mag in $(B - V)$ and $(V - I)$. Higher errors are seen in $(U - B)$.

Our CTIO final optical photometric catalogues consist of 4432, 8485, 12464, 1163 and 3892 entries having *UBVI* measurements down to $V \sim 22$ mag for ESO 131SC09, NGC 5284, VdB-Hagen 164, NGC 6268 and Czernik 38, respectively. As for LCO, the

© 2011 The Authors, MNRAS **419,** 3608–3623
Monthly Notices of the Royal Astronomical Society © 2011 RAS

Downloaded from http://mnras.oxfordjournals.org/ at Ural Federal University on March 27, 2015

Table 2. *UBVI* photometric observations of star clusters and standard star fields for the CTIO run.

Target	Date	Filter	Exposure (s)	Airmass
PG 1047	2006 May 21	*U*	90,180	1.15−1.25
		B	2 × 80	1.15−1.21
		V	2 × 50	1.14−1.16
		I	2 × 50	1.15−1.15
ESO 131SC09	2006 May 21	*U*	30, 200, 1500	1.13−1.13
		B	30, 100, 1200	1.14−1.16
		V	30, 100, 900	1.14−1.15
		I	30, 100, 700	1.13−1.14
NGC 5284	2006 May 21	*U*	30, 200, 1500	1.15−1.15
		B	30, 100, 1200	1.16−1.15
		V	30, 100, 900	1.15−1.15
		I	30, 100, 700	1.15−1.15
PG 1323	2006 May 21	*U*	2 × 150	1.15−1.14
		B	80	1.13−1.14
		V	50	1.15−1.15
		I	50	1.14−1.14
VdB-Hagen 164	2006 May 21	*U*	30, 200, 1500	1.25−1.25
		B	30, 100, 1200	1.26−1.25
		V	30, 100, 900	1.25−1.25
		I	30, 100, 700	1.25−1.25
NGC 6268	2006 May 21	*U*	30, 200, 1500	1.15−1.15
		B	30, 100, 1200	1.16−1.15
		V	30, 100, 900	1.15−1.15
		I	30, 100, 700	1.15−1.15
MarkA	2006 May 21	*U*	100, 150, 180	1.05−1.94
		B	3 × 80	1.03−1.84
		V	3 × 50	1.05−1.85
		I	3 × 50	1.04−1.99
Czernik 38	2006 May 21	*B*	30, 100, 1200	1.46−1.45
		V	10, 30, 100, 900	1.45−1.45
		I	30, 100, 700	1.45−1.45
G26	2006 May 21	*U*	100, 150	1.35−1.74
		B	2 × 80	1.33−1.77
		V	2 × 50	1.35−1.75
		I	2 × 50	1.34−1.79

catalogues for IC 2714, NGC 4052, NGC 5316 and NGC 5715 report 2756, 6650, 2524 and 4105 *UBVI* entries, respectively. These catalogues will be made available at the WEBDA[7] data base maintained by E. Paunzen at Vienna University, Austria.

3.5 Completeness and astrometry

Completeness corrections were determined by running artificial star experiments on the data. Basically, we created several artificial images by adding artificial stars to the original frames. These stars were added at random positions and had the same colour and luminosity distribution as of the true sample. To avoid overcrowding, in each experiment we added up to 25 per cent of the original number of stars. Depending on the frame, between 1000 and 5000 stars were added. In this way, we have estimated that the completeness level of our photometry is better than 90 per cent down to $V = 19.5$.

Each optical catalogue was then cross-correlated with 2MASS, which resulted in a final catalogue including *UBVI* and JHK_s magnitudes. As a by-product, pixel (i.e. detector) coordinates were converted into RA and Dec. for J2000.0 equinox, thus providing

[7] Available from http://www.univie.ac.at/webda/navigation.html

Table 3. *UBVI* photometric observations of star clusters and standard star fields for the LCO run.

Target	Date	Filter	Exposure (s)	Airmass
IC 2714	2010 May 08	*U*	10, 300, 1500	1.28−1.35
		B	10, 200, 1200	1.25−1.26
		V	3, 30, 900	1.23−1.23
		I	3, 10, 900	1.21−1.23
MarkA	2010 May 08	*U*	2 × 240	1.07−1.38
		B	2 × 180	1.07−1.41
		V	2 × 60	1.07−1.43
		I	40, 50	1.07−1.43
PG 1047	2010 May 08	*U*	20, 180	1.14−1.91
		B	15, 180	1.14−1.88
		V	2 × 10, 20, 30	1.15−1.83
		I	10, 30	1.15−1.86
PG 1323	2010 May 08	*U*	180	1.11−1.11
		B	120	1.12−1.12
		V	30	1.15−1.15
		I	30	1.14−1.14
NGC 4052	2010 May 09	*U*	10, 300, 1500	1.28−1.35
		B	10, 200, 1200	1.21−1.22
		V	3, 30, 900	1.23−1.24
		I	3, 10, 900	1.22−1.22
NGC 5316	2010 May 09	*U*	10, 300, 1500	1.17−1.20
		B	10, 200, 1200	1.22−1.22
		V	3, 30, 900	1.23−1.24
		I	3, 10, 900	1.19−1.19
MarkA	2010 May 09	*U*	240	1.30−1.30
		B	180	1.33−1.33
		V	60	1.28−1.28
		I	60	1.26−1.26
PG 1633	2010 May 09	*U*	90, 120	1.29−1.72
		B	60, 90	1.29−1.74
		V	30, 40, 90	1.29−1.76
		I	30, 40	1.29−1.78
PG 1323	2010 May 09	*U*	3 × 25, 60	1.07−1.88
		B	2 × 20, 26, 60	1.07−1.71
		V	10, 3 × 15, 2 × 30	1.07−1.79
		I	3 × 15, 30	1.07−1.74
NGC 5715	2010 May 10	*U*	10, 300, 1500	1.19−1.19
		B	10, 200, 1200	1.25−1.26
		V	3, 30, 900	1.19−1.20
		I	3, 10, 900	1.21−1.22
PG 1323	2010 May 10	*U*	2 × 25	1.07−1.22
		B	2 × 20	1.07−1.22
		V	2 × 10	1.07−1.20
		I	2 × 10	1.07−1.20
PG 1657	2010 May 10	*U*	2 × 180	1.29−1.49
		B	2 × 120	1.29−1.52
		V	2 × 60	1.30−1.54
		I	2 × 60	1.30−1.56

2MASS-based astrometry, useful for spectroscopic follow-up for example.

4 COMPARISON WITH PREVIOUS PHOTOMETRY

The only cluster in our sample having previous CCD photometry is Czernik 38, for which *BV* photometry was provided by Maciejewski (2008). We can only compare *BV*, since Maciejewski did not observe in *I*. We found 425 stars in common and the results are shown in Fig. 3, in the sense of our photometry excluding the observations of Maciejewski. We found that the two studies are much different in

Downloaded from http://mnras.oxfordjournals.org/ at Ural Federal University on March 27, 2015

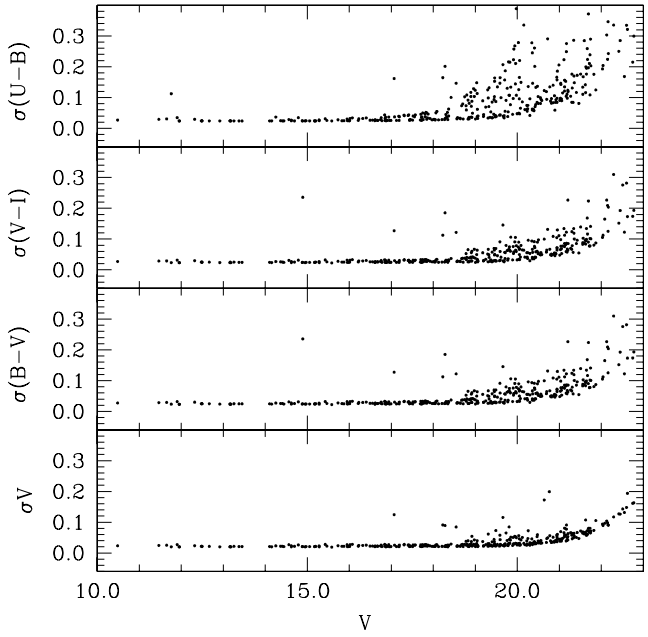

Figure 2. Photometric errors in V, $(B - V)$, $(V - I)$ and $(U - B)$, as a function of the V magnitude.

both the V and B magnitudes. The mean zero-point differences are reported in Fig. 3, which can be due to various reasons. Recall that Maciejewski observed in very poor seeing conditions (∼4 arcsec) and with a Schmidt camera having a scale as large as 1.08 arcsec pixel^{-1}. In addition, the colour range $(B - V)$ of the standard stars is limited between 0.3 and 1.3, while all main-sequence stars in Czernik 38 have redder colours. This implies that Maciejewski had to extrapolate colours when calibrating. Moreover, with such a poor detector scale, the seeing conditions and a moderate crowding of the field (see Fig. 1) easily produce blends, and stars tend on the average to be brighter. This is exactly what the positive residuals in

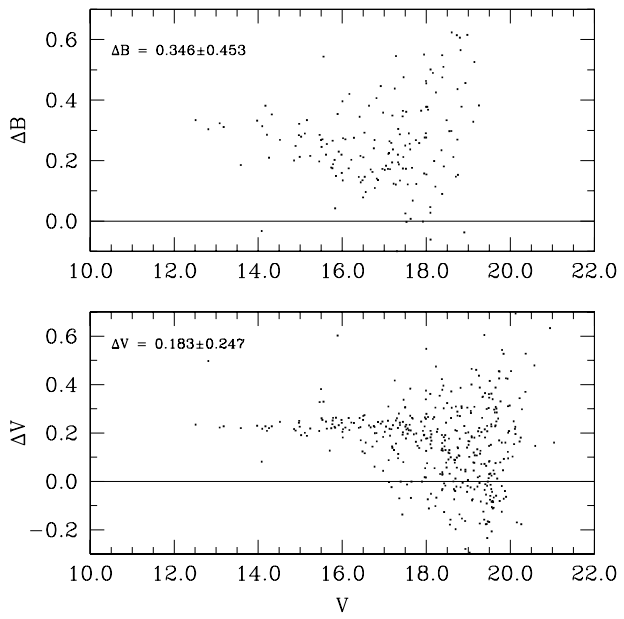

Figure 3. Comparison of our photometry for Czernik 38 with Maciejewski (2008) for V and B. The comparison is in the sense of our photometry versus that of Maciejewski (2008).

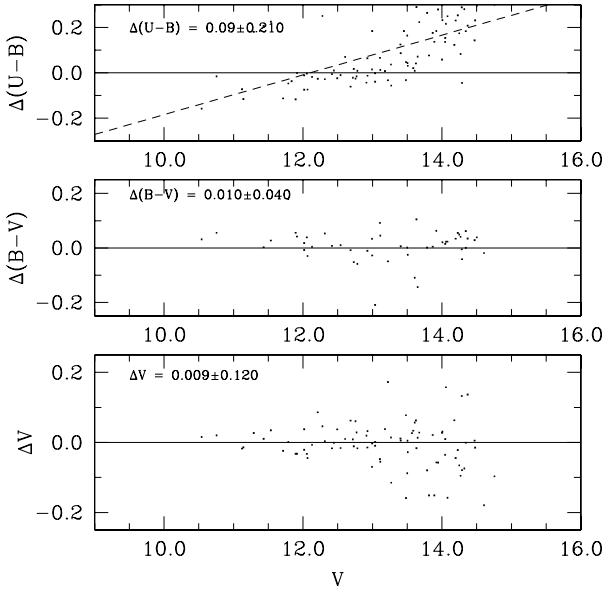

Figure 4. Comparison of our photometry for IC 2714 with Clariá et al. (1994) for $V, B - V$ and $U - B$. The comparison is in the sense of our photometry versus theirs.

Fig. 3 indicate. For all these reasons, we believe that our photometry is more solid and precise (note the scatter in the residual in Fig. 3 for V larger than ∼17.0 mag).

To further check the quality of our data, we compared our *UBV* photometry for IC 2714 with a higher quality photoelectric study by Clariá et al. (1994), as shown in Fig. 4. The comparison is performed for 90 common stars and is in the sense of our photometry excluding the observations of Clariá et al. (1994). The results are quite good for V and $B - V$, as indicated in Fig. 4, down to $V \sim 14.0$. However, we found some discrepancy for $U - B$, in the form of an unaccounted colour term.

5 STAR COUNTS, CLUSTERS' REALITY AND SIZE

In this section, to perform star counts in the area of the programme clusters, assess their reality and derive estimates of their radii, we make use of our photometric data set and infrared photometry from the 2MASS data base.

5.1 Surface density maps and cluster centre coordinates

Surface density maps (SDMs) were constructed for all fields under investigation to determine the reality and size of the cluster. Examples of the application of this technique can be found in Prisinzano et al. (2001), Pancino et al. (2003) and Seleznev et al. (2010) We refer the reader to these papers for further details.

Briefly, SDMs were constructed using the kernel estimation method (see e.g. Silverman 1986), with a kernel half-width of 400 pixels (corresponding to 2.90 arcmin for LCO clusters and 1.93 arcmin for CTIO clusters). Moreover, a grid of 20-pixel cells for LCO clusters and a grid of 50-pixel cells for CTIO clusters were adopted. The large kernel half-width was chosen in order to both decrease the effect of density fluctuations (to avoid, for example, numerous unreal density peaks inside a cluster) and detect the cluster centre more clearly. Only stars brighter than a specific magnitude

Downloaded from http://mnras.oxfordjournals.org/ at Ural Federal University on March 27, 2015

Table 4. Limiting magnitude for star counts in optical.

Label	Name	Limit in V
1	IC 2714	16
2	NGC 4052	16
3	ESO 131SC09	17
4	NGC 5284	17
5	NGC 5316	16
6	NGC 5715	16
7	VdB-Hagen 164	17
8	NGC 6268	17
9	Czernik 38	19

limit – depending on the field – were considered since the inclusion of faint stars has sometimes the effect of confusing the cluster inside the rich surrounding back-/foreground. These limiting magnitudes are listed in Table 4.

To avoid undersampling, we only made use of the 1240 × 2340 pixel (∼9.0 × 17.0 arcmin^2) central region for LCO clusters and of the 3250 × 3250 pixel (∼15.7 × 15.7 arcmin^2) central region for CTIO clusters. The resulting SDMs are shown in Fig. 5, where the isodensity contour lines are in units of (100 pixel)$^{-2}$.

New rough coordinates for the cluster centres were obtained from the centre of symmetry of the inner (maximum) density contours. In the cases of irregular structures, we estimated centre position through comparison with 2MASS density maps (see the discussion below). The new cluster centres' coordinates are listed in Table 5 and indicated by crosses in Fig. 5. We emphasize that the use of more sophisticated methods for cluster centre determination would not make much sense in this case, because the position of the cluster centre clearly depends on both the limiting magnitude and kernel half-width. Table 5 also contains rough estimates of radii for the denser central regions of the clusters (cores).

One can clearly note that in most cases the cluster size is larger than the detector FOV or just comparable to it. Therefore, in order to study the cluster structure in larger areas, to plot density profiles and

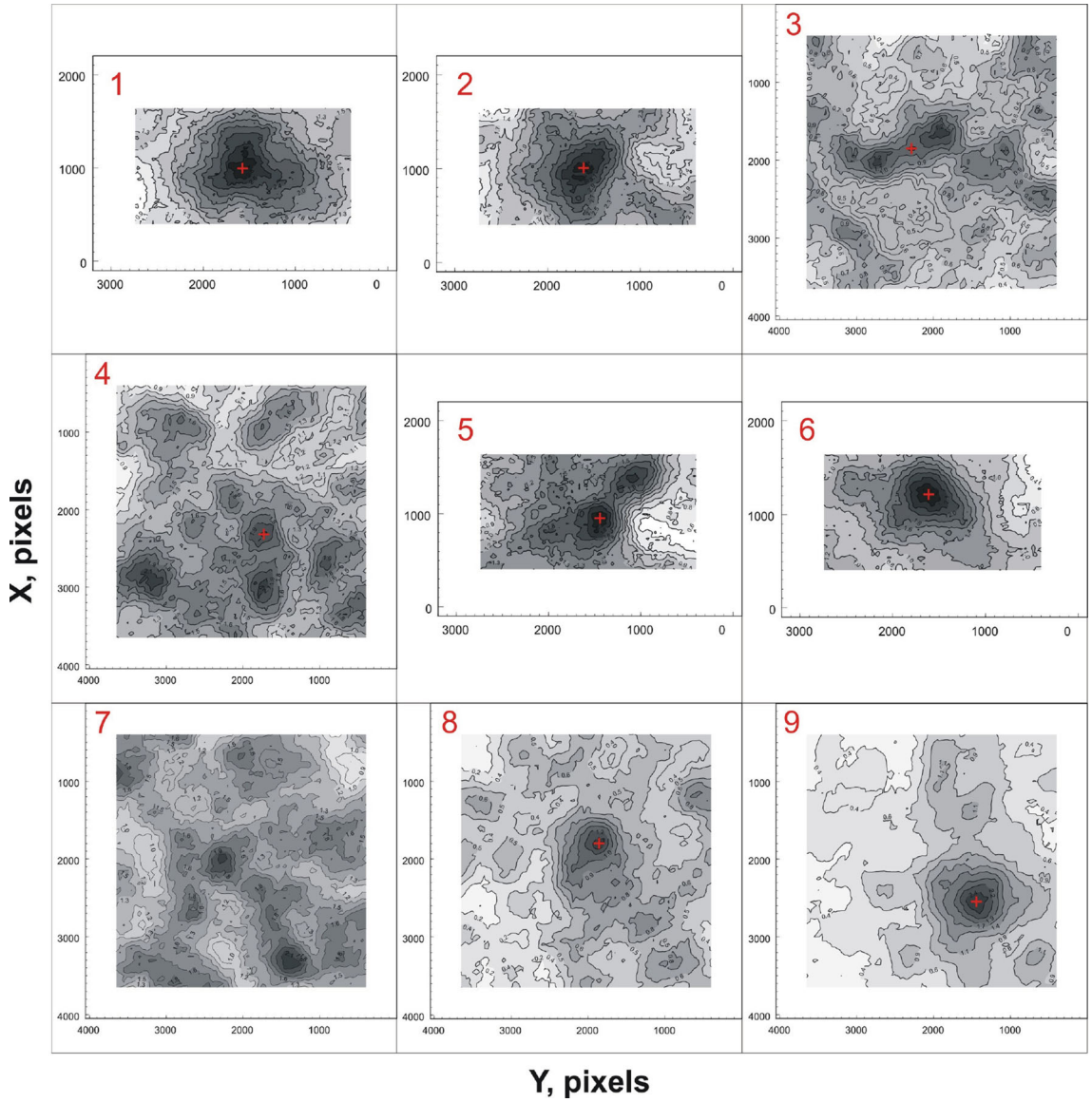

Figure 5. Optical SDMs for the nine programme clusters. North is right and east is down. Numbering follows as in Table 1.

Downloaded from http://mnras.oxfordjournals.org/ at Ural Federal University on March 27, 2015

Table 5. Centre coordinates and core radii in pixels of the nine clusters under study.

Label	Name	X_c (pixels)	Y_c (pixels)	'Core' radius (pixels)	Comments
1	IC 2714	1000	1570	1000	
2	NGC 4052	1000	1600	800	
3	ESO 131SC09	1860:	2280:	900	Two centres
4	NGC 5284	2300:	1720:	1050	Complicated structure
5	NGC 5316	950	1450	800	
6	NGC 5715	1200	1600	600	
7	VdB-Hagen 164	–	–	–	
8	NGC 6268	1800	1830	600	
9	Czernik 38	2550	1450	700	

to estimate cluster sizes, we made use of star counts of photometry from the 2MASS data base.

5.2 2MASS SDMs and radial surface density profiles for sample clusters

Nine fields of 3600 × 3600 arcsec (boxes) centred on clusters were downloaded from the 2MASS data base. These fields contain a large number of stars, and SDMs are plotted taking into account all stars to show density fluctuations which mask the clusters completely. In order to make clusters more evident, SDMs were plotted for stars selected on colour–magnitude diagrams (CMDs). Stars were selected in intervals of $(J - H) \simeq \pm 0.15$ wide around the position of isochrones' set superimposed on the CMD and using preliminary values of reddening and distance modulus, mostly based on visual inspection.

SDMs obtained with kernel half-width of 5 arcmin and a grid of 0.5-arcmin cells are shown in Fig. 6. Limiting magnitudes of stars were selected in order to make clusters as visible as possible, and these limiting magnitudes are listed in Table 6 (third column).

To guide the reader, white rectangles in Fig. 6 show position and extent of optical FOVs. These positions were obtained by cross-identification of the brightest stars in the optical and infrared fields. All clusters clearly stand out except for VdB-Hagen 164. This cluster, which has been taken from the list of van den Berg & Hagen (1975), if real, is probably very poorly populated, close, very sparse with an angular size of supposedly much more than 1°. The data we have analysed, however, do not give us the impression of a cluster, and therefore we consider it as a false detection in this paper (see the following sections).

SDMs for all the clusters were obtained for different limiting magnitudes. A close analysis of these maps shows that the cluster centre position depends on the limiting magnitude. Table 7 shows coordinates of 2MASS fields and cluster centre positions with respect to the field centre (telescope pointing): $\alpha_c = \alpha + \Delta\alpha$, $\delta_c = \delta + \Delta\delta$ (corrections are given in arcmin). Each limiting magnitude correction is given in the order of $\Delta\alpha/\Delta\delta$.

Radial surface density profiles (RSDPs) – $F(r)$ – were then obtained by using the kernel method and adopting a kernel half-width of 2 arcmin. The kernel size was adjusted to avoid both extra smoothing and irregularities. RSDPs are shown in Fig. 7 as solid curves with points. Solid curves show a 1σ confidence interval, which is obtained using a 'smoothed bootstrap' algorithm (see e.g. Seleznev et al. 2010 and Prisinzano et al. 2001 for more details). Solid polygonal lines show density histograms with steps of 1 arcmin. The adopted limiting magnitudes for RSDPs are listed in the fourth column of Table 6. Finally, $F(r)$ is shown in units of $(\text{arcmin})^{-2}$.

By inspecting Fig. 7, one can note the small values of $F(r)$ at the cluster centres' position in a few cases. These are due to irregularities in the field caused, in some cases, by patchy extinction and/or field density fluctuations. Technically, the reason is that the cluster centres were determined from SDMs constructed with a large kernel half-width (5 arcmin), whereas RSDPs have been derived adopting smaller values for the kernel width. The smaller scale produces a fluctuating profile and, as a consequence, low density values can be obtained at the centres when $F(r)$ is constructed using small increments.

5.3 Results from the SDM and RSDP analysis

In this section, we analyse the outcome of star counts on a cluster-by-cluster basis, highlighting the most important results.

IC 2714. This is a rich cluster with an angular radius of about 19 arcmin. The cluster manifests a relatively regular structure for $J_{\rm lim} = 13$, which became more irregular for $J_{\rm lim} = 15$. However, at $J_{\rm lim} = 16$ (the limit of 2MASS completeness), the cluster disappears against background density fluctuations.

NGC 4052. This cluster has an angular radius of about 14 arcmin. It is clearly seen in the SDMs down to $J_{\rm lim} = 14$. When including fainter stars, the cluster is still visible, but looks less populous than neighbour density fluctuations. 'Optical' SDM shows a double core and an elongated outer core region.

ESO 131SC09. This is a small group with an angular radius of about 4 arcmin. SDM shows two neighbour density fluctuations, 9 arcmin to the south and about 8 arcmin to the north-west, respectively. To address the question of whether they are part of the cluster, one needs additional information, e.g. proper motions. The *optical* SDM shows elongation of the cluster roughly in the north–south direction and the presence of several density peaks. The position of the cluster centre was conservatively taken as the small peak just in between the two more general density peaks. In the 2MASS SDM, the cluster is visible down to $J_{\rm lim} = 14$ and disappears when fainter stars are included against the background density fluctuations.

Interestingly enough, the star density peak has a very low contrast with the field, the lowest in our sample. This fact may indicate that the central peak can be caused by an interstellar absorption minimum.

NGC 5284. This cluster has a complex structure. At $J_{\rm lim} = 13$ and 14, SDMs show a double structure with the second component 8 arcmin to the east. At $J_{\rm lim} = 15$, the second component disappears, but we see another component 13 arcmin apart in the north-east direction. At $J_{\rm lim} = 16$, this component becomes prominent. The

Downloaded from http://mnras.oxfordjournals.org/ at Ural Federal University on March 27, 2015

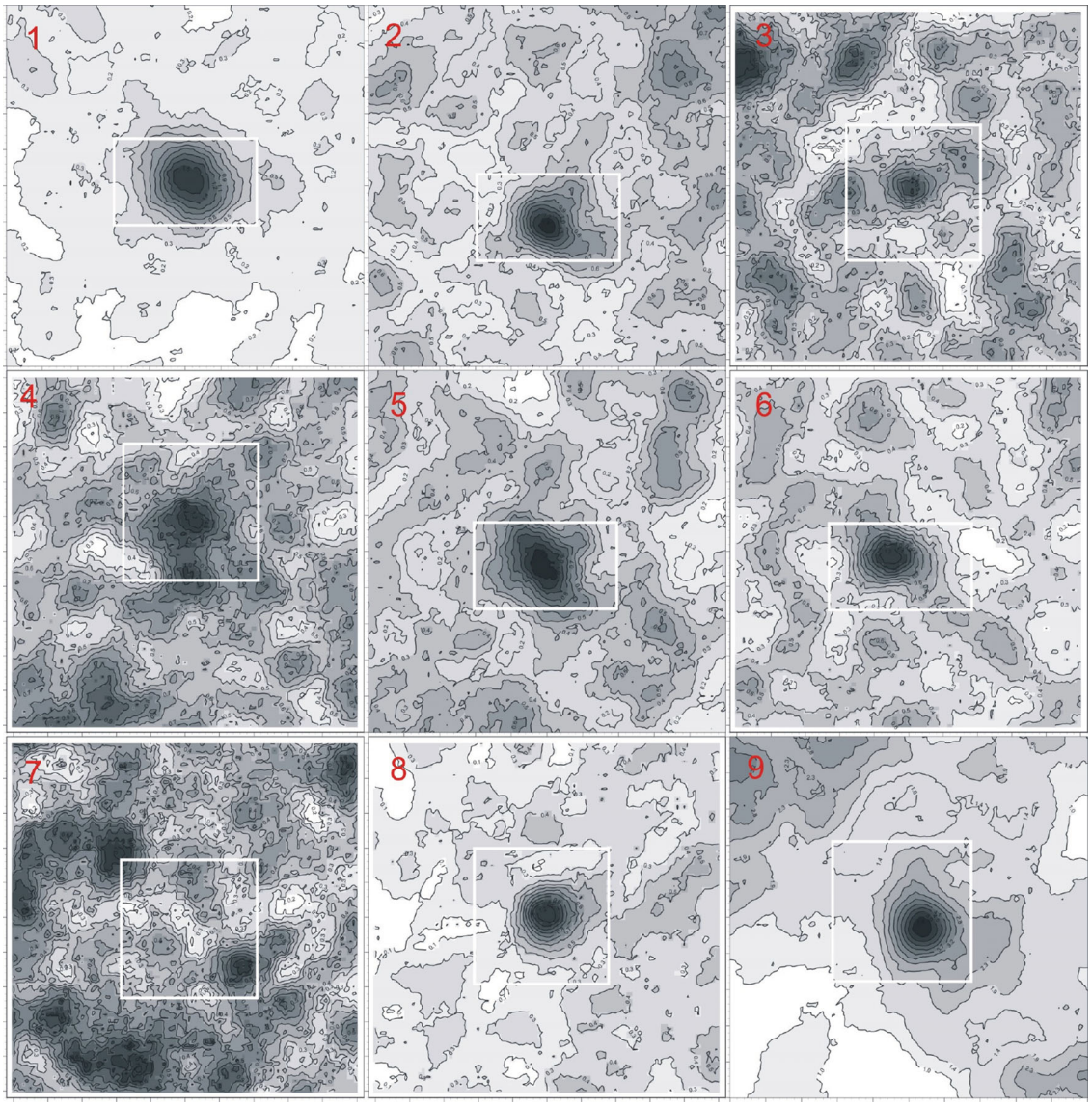

Figure 6. 2MASS SDMs for the nine programme clusters. North is right and east is down. White boxes enclose the area covered by optical data. Numbering follows as in Table 1.

Table 6. Limiting magnitudes for density maps from 2MASS.

Label	Name	SDM limit in J	RSDP limit in J
1	IC 2714	13	15
2	NGC 4052	13	16
3	ESO 131	12	14
4	NGC 5284	13	15
5	NGC 5316	13	15
6	NGC 5715	13	16
7	BH 164	13	
8	NGC 6268	13	16
9	Cz 38	15	16

optical SDM also shows a complex structure with several secondary maxima. The RSDP gives a cluster radius estimate of about 17 arcmin.

NGC 5316. This cluster stands out neatly in SDMs for $J_{\rm lim} = 13$ and 14. At $J_{\rm lim} = 15$, the cluster is still visible, but we see comparable density fluctuations around them. At $J_{\rm lim} = 16$, the cluster disappears against the background density fluctuations. The RSDP suggests a cluster radius of about 9 arcmin. The optical SDM shows an asymmetric complex structure with at least two secondary density maxima.

NGC 5715. This cluster is well defined for all limiting magnitudes. At $J_{\rm lim} = 14$, it exhibits a double structure. Neighbour density fluctuations become stronger when including fainter stars. RSDP gives a cluster radius estimate of about 8 arcmin.

VdB-Hagen 164. This cluster was listed by van den Berg & Hagen (1975). It does not possess a clear density peak either in 'optical' or in 'infrared' SDMs. The authors observed that the cluster is visible in blue plates and invisible in red plates. Possibly, it is a sparse group of young stars with an angular size of about a degree or even more. However, SDMs plotted for a 2 × 2 deg large field do not show any density peak either.

NGC 6268. This cluster is clearly defined for all limiting magnitudes. Density fluctuations grow with increasing limiting magnitude and concentrate in the north-west quadrant with respect

Downloaded from http://mnras.oxfordjournals.org/ at Ural Federal University on March 27, 2015

Table 7. New equatorial coordinates for the clusters under investigation, obtained using 2MASS-based SDMs.

Label	Name	RA ($^{h\ m\ s}$)	Dec. ($^{\circ}\ '\ ''$)	$J < 12$	$J < 13$	$J < 14$	$J < 15$	$J < 16$	Comments
1	IC 2714	11:17:30	−62:44:00		−0.6/+0.5	−1.0/+0.3	−0.5/+1.0		
3	ESO 131	12:29:38	−57:52:36	+1.0/+0.5	+1.0/+0.6	+0.1/+0.6			
2	NGC 4052	12:01:12	−63:13:00		+5.8/+0.1	+5.0/−0.1	+4.5/−0.1	+4.0/−0.5	
4	NGC 5284	13:47:23.3	−59:08:58		−4.2/+1.1	−3.8/+0.8	−2.4/+0.5	−1.3/−2.3*	*2nd centre became main
5	NGC 5316	13:53:54	−61:52:00		+2.0/−0.7	+3.0/−0.5	+4.4/−0.1		
6	NGC 5715	14:43:24	−57:33:00		+0.9/−2.5	+1.0/−2.5	+1.0/−2.5	0.0/−2.2	
7	BH 164	14:48:14	−66:20:23	–	–	–	–	–	
8	NGC 6268	17:02:10	−39:43:42		−0.3/−0.1	−0.2/+0.2	−0.1/+0.3	+0.2/0.0	
9	Cz 38	18:49:42	04:56:00		+2.4/+2.1	+1.5/+2.0	+1.5/+2.0	+1.1/+1.8	

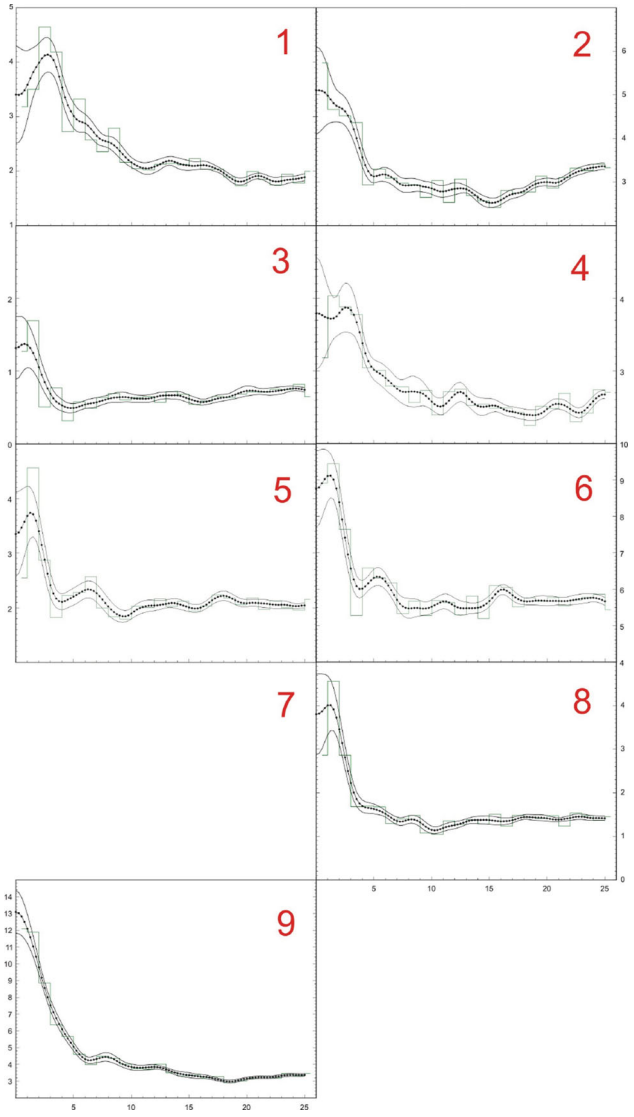

Figure 7. Surface radial density profiles for the nine programme cluster. Numbering follows as in Table 1. No profile is shown for VdB-Hagen 164 (see Section 5).

to the cluster. RSDP gives a cluster radius estimate of about 10 arcmin.

Czernik 38. This is a relatively rich cluster with an angular radius of about 16–18 arcmin. It has a symmetric core and a slightly asymmetric halo elongated in the north direction. The RSDP of this cluster shows a 'step' near $r = 8$ arcmin.

6 FUNDAMENTAL PARAMETERS: REDDENING, DISTANCE AND AGE

In this section, we make use of the results of the star count analysis to derive estimates of the fundamental parameters, namely reddening, distance and age, for the clusters under study.

6.1 Basics of the method

We only considered the stars that fall inside the core radius, as defined in previous sections, with the aim of alleviating as much as possible field star contamination and render the cluster more visible. First, to derive an independent estimate of the cluster mean reddening, the method employed is based on the inspection of the colour–colour diagram (TCD) in the $B - V$ versus $U - B$ colour combination. In this diagram, the position of stars with spectral types earlier than A0 depends only on reddening (Carraro, Moitinho & Vázquez 2008). Then, the analysis moves on to the inspection of the CMDs, in various colour combinations, to derive estimates of the cluster distance and age. For the sake of homogeneity with previous studies (e.g. Seleznev et al. 2010), we adopt $R_{\odot} = 8.5$ kpc as the distance of the Sun to the Galactic Centre and $R_V = 3.1$ as the ratio of the total to selective absorption $A_V/[E(B - V)]$. Finally, note that we adopt solar metallicity for these clusters, as a working hypothesis, when no information is available from spectroscopy. This is partly justified by the clusters' location in the inner disc. Should solar metallicity clearly be unsuitable, we will then explore different values.

6.2 Error analysis

With the probable exception of IC 2714, most clusters in this paper are studied for the first time. We, therefore, face the well-known problem of associating reliable errors to distance and age. Without precise estimates of reddening and metallicity, it is extremely difficult to perform a proper error assessment. This would imply, in theory, a full error propagation which would, in general, produce a very large inner volume in the parameters' space with many solutions which would not pass a simple by-eye inspection.

We will, therefore, limit ourselves to providing fitting errors for the cluster reddening and apparent distance moduli, being totally aware that they most probably are only rough lower limits awaiting improvements as soon as more precise metallicity measurements will be available. However, in deriving distance, a full propagation is done taking into account the whole range of values for reddening and distance modulus. Finally, as far as the ages are considered, only fitting errors are reported, adopting solar metallicity (see below).

Downloaded from http://mnras.oxfordjournals.org/ at Ural Federal University on March 27, 2015

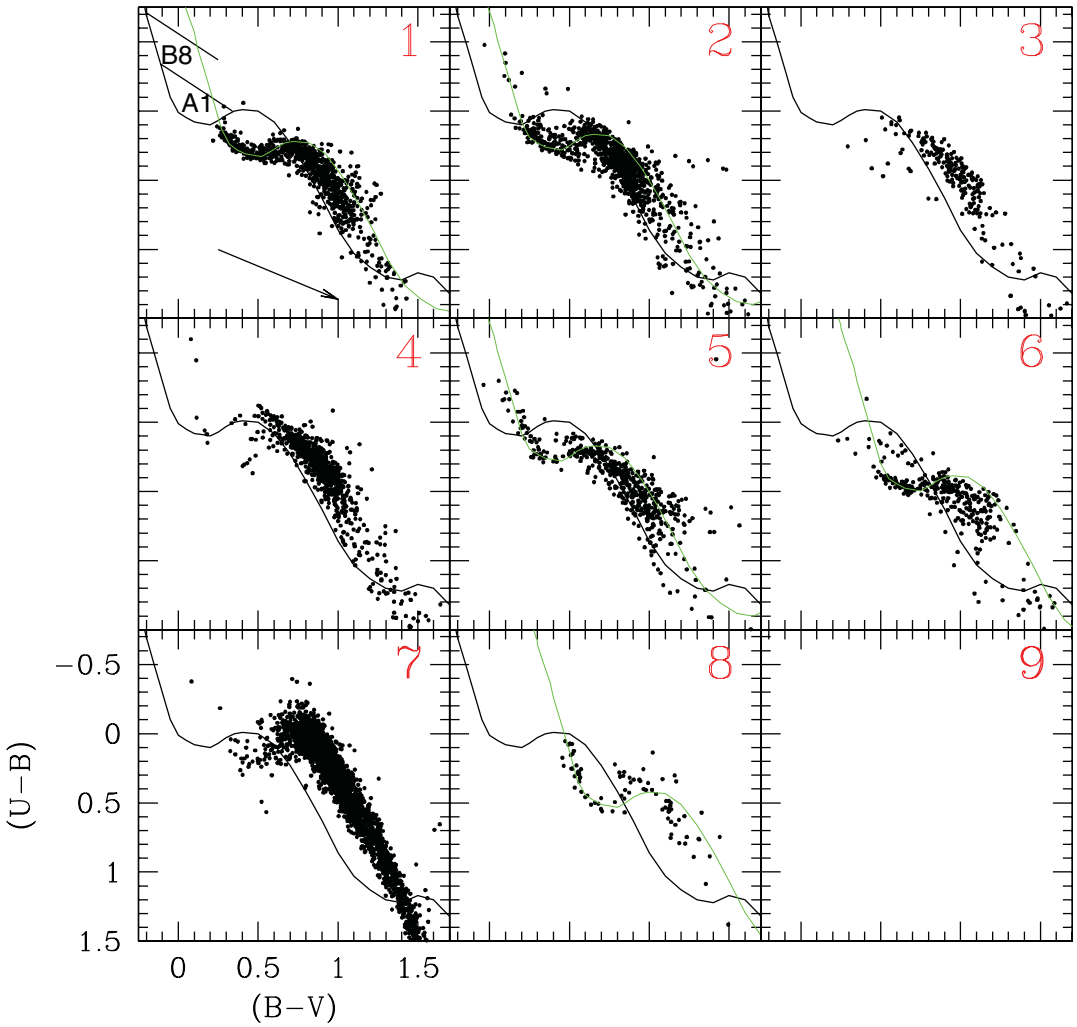

Figure 8. Colour–colour diagrams for the nine programme clusters. The numbering follows as in Table 1. The solid line is an empirical zero-reddening ZAMS. The arrow in the top-left panel indicates the reddening vector. Two spectral types are indicated to guide the eye, together with the reddening path. The green line is the same as ZAMS, but shifted along the reddening path by an amount corresponding to the cluster reddening $E(B-V)$.

6.3 Clusters' reddening

In Fig. 8 we show the TCDs for eight of the nine programme clusters. Unfortunately, we could not provide U-band photometry for Czernik 38 and therefore we estimate its reddening simultaneously with age and distance from the CMD analysis, using theoretical isochrones, in a less effective way (see below). Fig. 8 shows the TCD for the programme clusters following their numbering as in Table 1. As anticipated, only stars within the core radius are used. The solid line is a zero-reddening, solar metallicity, empirical zero-age main sequence (ZAMS) taken from Schmidt-Kaler (1982). In each panel, the same empirical ZAMS is shifted along the reddening vector (indicated by the arrow in the upper-left corner) to fit the bulk of the stars in each cluster, using the green colour, whenever possible. As for the fit, this is done by considering only the stars with a spectral type earlier than A0, since for later spectral type stars no unique fitting solution exists. To facilitate viewing, we indicated two spectral types along the ZAMS and the paths, parallel to the reddening vector, along which stars are displaced by reddening.

This procedure allows us to estimate the mean reddening for each cluster, as reported in Table 8 (third column). The associated uncertainties have been estimated visually and represent the range in reddening we can move back and forth the ZAMS keeping the fit acceptable. This uncertainty basically comes from photometric errors and variable reddening across the cluster. When the uncertainty is larger than photometric errors, which are much less than 0.03 mag in this magnitude range (see Fig. 2), we are forced to conclude that differential reddening is present in the cluster. This is far from being unexpected, since these clusters are typically located at low latitude in the inner Galactic disc, inside or close to gas- and dust-rich spiral features.

6.4 Clusters' distance and age

Distances are estimated in the CMDs in Figs 9–11, using the same ZAMS as in the previous section, and adopting the reddening values already derived. In this process, therefore, distance is the only free parameter, having fixed metallicity and reddening. In the same way as for reddening, the uncertainty in distance is estimated shifting the ZAMS (green line) vertically for the range of distance moduli which provides an acceptable fit. Note that in this process the reddening remains within the range of values independently estimated in the TCD.

Downloaded from http://mnras.oxfordjournals.org/ at Ural Federal University on March 27, 2015

Table 8. Estimates and associated uncertainties of the fundamental parameters of the clusters under study.

Number	Name	$E(B-V)$ (mag)	$(m-M)_V$ (mag)	Age (Myr)	$d_\odot$ (kpc)	d_{GC} (kpc)	z (pc)
1	IC 2714	0.33 ± 0.05	11.60 ± 0.10	300 ± 20	$1.30^{+0.10}_{-0.15}$	8.1	~ 40
2	NGC 4052	0.30 ± 0.05	12.70 ± 0.20	400 ± 40	$2.20^{+0.50}_{-0.30}$	7.8	~ 30
3	ESO 131SC09						
4	NGC 5284						
5	NGC 5316	0.25 ± 0.05	11.50 ± 0.20	100 ± 10	$1.40^{+0.15}_{-0.20}$	7.6	~ 0
6	NGC 5715	0.55 ± 0.10	12.75 ± 0.20	500 ± 100	$1.60^{+0.80}_{-0.50}$	7.4	~ 60
7	VdB-Hagen 164						
8	NGC 6268	0.40 ± 0.03	11.40 ± 0.20	150 ± 10	$1.07^{+0.20}_{-0.10}$	7.1	~ 20
9	Czernik 38	1.25 ± 0.10	15.30 ± 0.20	600 ± 100	$1.90^{+0.55}_{-0.40}$	7.2	~ 80

The final step is to estimate the age, and for this we make use of isochrones from the Padova suite of models (Marigo et al. 2008; red symbols). When fitting isochrones, we pay attention to the turn-off (TO) colour, magnitude and shape and, when present, to the red giant clump colour and magnitude. In addition, we require that the fit is of the same quality in all the three colour combination CMDs. The results are summarized in Table 8 and illustrated in Figs 9–11.

7 DISCUSSION

Having provided details on how fundamental parameter estimates are searched, we now discuss each individual cluster, commenting on the specific results. In fact, while in general a homogeneous technique has been applied, some cases, such e.g. Czernik 38, do require more information.

IC 2714. The set of fundamental parameters we found for this cluster is in good agreement with that of Clariá et al. (1994) within the uncertainties, in spite of the colour term problem we found while comparing their photoelectric photometry with our CCD data set. Our results are shown in the bottom panels of Fig. 9. The TO point is located at $V \sim 12.5$, $(B-V) \sim 0.30$ and $(V-I) \sim 0.40$. A sparse red giant clump is visible at $V \leq 12.0$, $(B-V) \geq 1.2$. Santos et al. (2009) derived spectroscopic iron abundance of three giants and provided for IC 2714 [Fe/H] $= 0.02 \pm 0.01$ and [Fe/H] $= -0.01 \pm 0.01$, depending on the line list used. In any case, metallicity is very close to solar.

We, therefore, searched the solar metallicity isochrone which best fits the distribution of cluster star in the CMD and obtained an age of $3.0 \pm 0.2 \times 10^8$ yr. This implies an apparent distance modulus of $(m-M)_V = 11.6 \pm 0.1$. At the corresponding heliocentric distance of $1.3^{+0.10}_{-0.15}$ kpc and ∼40 pc below the Galactic plane, IC 2714 is most probably about to leave the Carina arm, where it formed. To assess this scenario, we derived Galactic heliocentric velocities for IC 2714 from the literature. The cluster has a radial velocity of $R_V = -13.54 \pm 0.50$ km s^{-1} (Mermilliod, Mayor & Udry 2008) and UCAC2 proper motions $\mu_\alpha \cos\delta = -7.55 \pm 0.10$ and $\mu_\delta = 0.49 \pm 0.10$ (Dias et al. 2006). From these values, we derived $U = 34.43 \pm 3.18$ km s^{-1}, $V = 262.51 \pm 6.09$ km s^{-1} and $W = 14.41 \pm 1.53$ km s^{-1}, where U is positive towards the anticentre direction, V is positive in the Galactic rotation sense and W points towards the North Galactic Pole. The velocities we derive imply that the cluster is moving apart from the Carina arm, drifting towards larger Galactocentric distances.

NGC 4052. The middle panels of Fig. 9 show our results for NGC 4052, and the estimates of its basic parameters are listed in Table 8. The cluster TO is located at $V \sim 13.5$, $(B-V) \sim 0.30$ and $(V-I) \sim 0.40$, while a sparse red clump is at $V \sim 12.5$and $B-V \sim 1.2$. We fit the cluster sequence with a solar metallicity of 400 Myr isochrone and the Schmidt-Kaler (1982) ZAMS, which both yield an apparent distance modulus of $(m-M)_V = 12.7 \pm 0.2$.

As a consequence, NGC 4052 is located at $2.2^{+0.50}_{-0.30}$ kpc from the Sun and at 7.8 kpc from the Galactic Centre.

ESO 131SC09. Star counts reveal the presence of a concentration of stars at the position of this object. However, from the inspection of photometric diagrams, we are keen to derive a different conclusion (see Fig. 9, upper panels). Basically, we recognize two distinct groups of stars. A small number of bright blue stars in the upper region of the CMD is in fact superimposed to a larger group of F–G stars most probably belonging to the general Galactic disc field. The two groups are clearly separated in the CMDs, and such a significant magnitude gap excludes the fact that both groups belong to the same system. The apparent concentration in the maps is produced by the small group of bright stars which, evidently, do not define any stellar cluster, but, maybe, an open cluster remnant following the Loden's (1973) original definition (see also Platais, Kozhurina-Platais & van Leeuwen 1998; Carraro 2006). For these reasons, we refrain from trying any isochrone fitting.

NGC 5284. As star counts showed, this is a star agglomerate with a complicated structure. On DSS or CCD images, the cluster does not appear at all, and the CMDs shown in the bottom panels of Fig. 10 do not show convincingly the presence of a star cluster. We believe the overdensity is produced by a random concentration of a few blue stars, brighter than $V = 13$. As in the case of the previous cluster, this group looks like an open cluster remnant. In most cases, these groups do not turn out to be real clusters when proper motions or radial velocities are available to assess individual star membership to a cluster, as demonstrated by e.g. Odenkirchen & Soubiran (2002), Villanova et al. (2004), Carraro, Méndez & Costa (2005a) and Moni Bidin et al. (2010). Therefore, as in the case of ESO 131SC09, we refrain from trying any isochrone fitting.

NGC 5316. The CMDs for this cluster are shown in the middle panels of Fig. 10. The cluster is confirmed to be a physical group of young stars, with stars having spectral types as early as B5–B7. We use the reddening estimated in Fig. 8 and fit the CMDs with solar metallicity isochrones. The best fit is achieved with an age of 100 Myr, which, in turn, provides an apparent distance modulus of $(m-M)_V = 11.50 \pm 0.20$. Therefore, we place NGC 5316 at a heliocentric distance of $1.4^{+0.15}_{-0.20}$ kpc and a Galactic Centre distance of 7.6 kpc. This cluster lies very close to the formal Galactic plane at Galactic latitude $b = 0^\circ$.

Downloaded from http://mnras.oxfordjournals.org/ at Ural Federal University on March 27, 2015

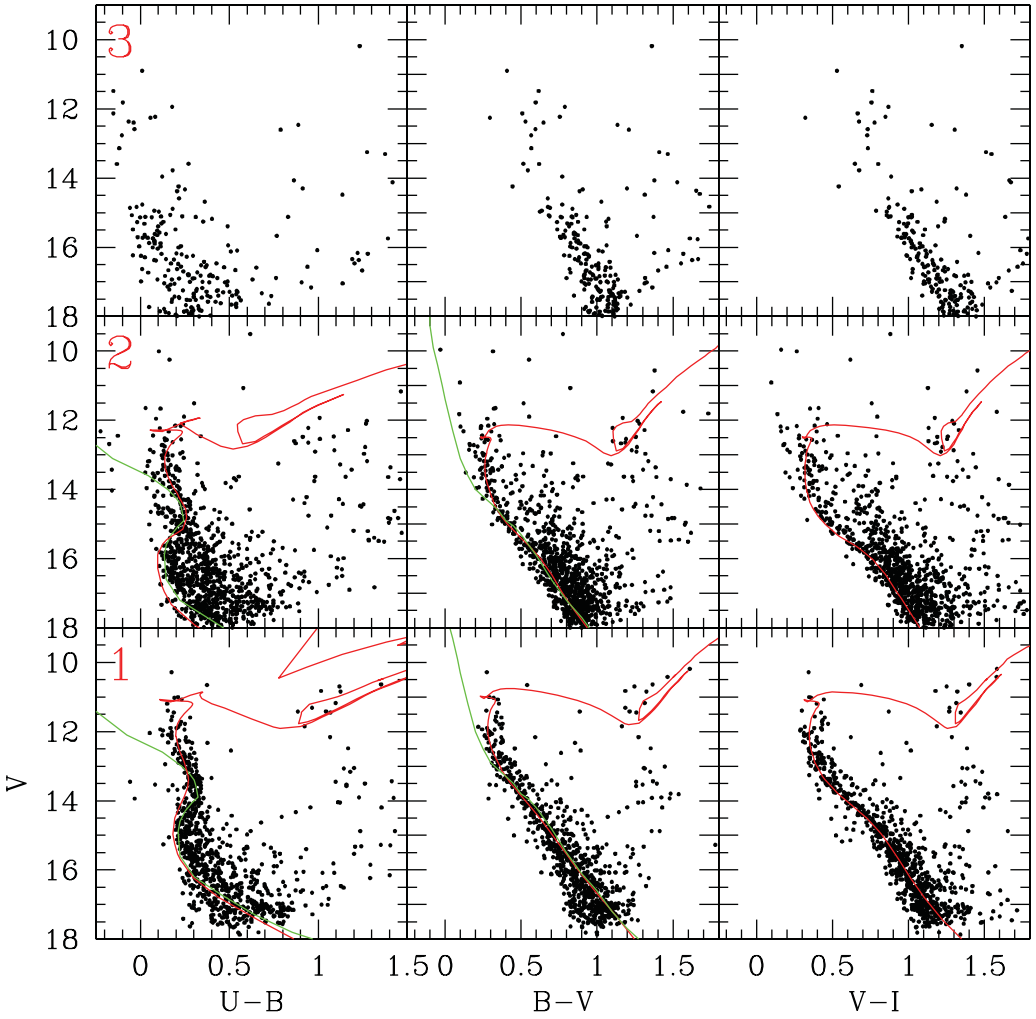

Figure 9. CMDs in the $V/U-B, V/B-V$ and $V/V-I$ for IC 2714, NGC 4052 and ESO 131SC09. Numbering follows as in Table 1. The green line is an empirical ZAMS shifted by an amount corresponding to the apparent distance modulus to fit the cluster sequence. The red lines are isochrones from Marigo et al. (2008).

NGC 5715. The CMDs of NGC 5715 (upper panels of Fig. 10) clearly indicate that it is an intermediate-age cluster, with a populated clump of red giant branch (RGB) stars at $V \sim 13.0$–13.5 and $(B-V) \sim 1.5$. The TO is located at $V \sim 14.0, (B-V) \sim 0.5$ mag. Adopting the reddening derived from Fig. 8, we found that an 500-Myr isochrone for solar metallicity nicely follows the star distribution in all the three colour combination CMDs. We estimate an apparent distance modulus of $(m-M)_V = 12.75 \pm 0.20$, which translates into a distance of $1.6^{+0.8}_{-0.5}$ kpc from the Sun. NGC 5715 is thus a Hyades-like cluster located in the inner disc, similar to NGC 6583 and NGC 6404 (Carraro et al. 2005b), which apparently survived long in spite of the difficult environment of these Galaxy regions.

VdB-Hagen 164. As already underlined in Section 5, there is no evidence of a star concentration neither in optical nor in infrared at the nominal position of this object. The absence of a star cluster is also obvious when inspecting CMDs (see Fig. 11, lower panels), since no clear sequences are seen in any of the diagrams. We conclude then that VdB-Hagen 164 is not a star cluster, but a random concentration of a few bright stars. As in the case of ESO 131SC09 and NGC 5284, we therefore refrain from trying any isochrone fitting.

NGC 6268. This looks like a small, compact and young cluster. The two-colour diagram reveals stars of the spectral type as early as B2. Using the reddening derived from this diagram, we fit the star distribution in the CMDs using a 150-Myr, solar metallicity, isochrone, using the same distance modulus as for the empirical ZAMS. The TO is located at $V \approx 11.5, (B-V) = 0.3$ and $E(V-I) = 0.4$ mag. There is no indication of an RGB clump. The fit looks fine and yields an apparent distance modulus of $(m-M)_V = 11.4 \pm 0.2$, which implies a heliocentric distance of $1.07^{+0.20}_{-0.10}$ kpc. The cluster is about 20 pc above the plane, and 7.1 kpc from the Galactic Centre. Its position is compatible with it being part of the Carina–Sagittarius arm.

Czernik 38. As commented earlier, we did not take U-band observations for this cluster, since it looked to be heavily reddened. The CMDs are shown in the upper panel of Fig. 11. The TO is located at $V = 16.5, (B-V) = 1.4$ and $(V-I) \sim 1.7$. A group of red stars at $V \sim 17.0$ seemingly indicates the presence of a RGB clump. We derived distance, age and reddening simultaneously by fitting a 600 Myr, solar metallicity, isochrone, which nicely follows the star distribution in the CMD. This fit returns a reddening $E(B-V) = 1.35 \pm 0.15$, and an apparent distance modulus $(m-M)_V = 15.30 \pm 0.20$. Therefore, we position Czernik 38 at $1.9^{+0.55}_{-0.40}$ kpc

Downloaded from http://mnras.oxfordjournals.org/ at Ural Federal University on March 27, 2015

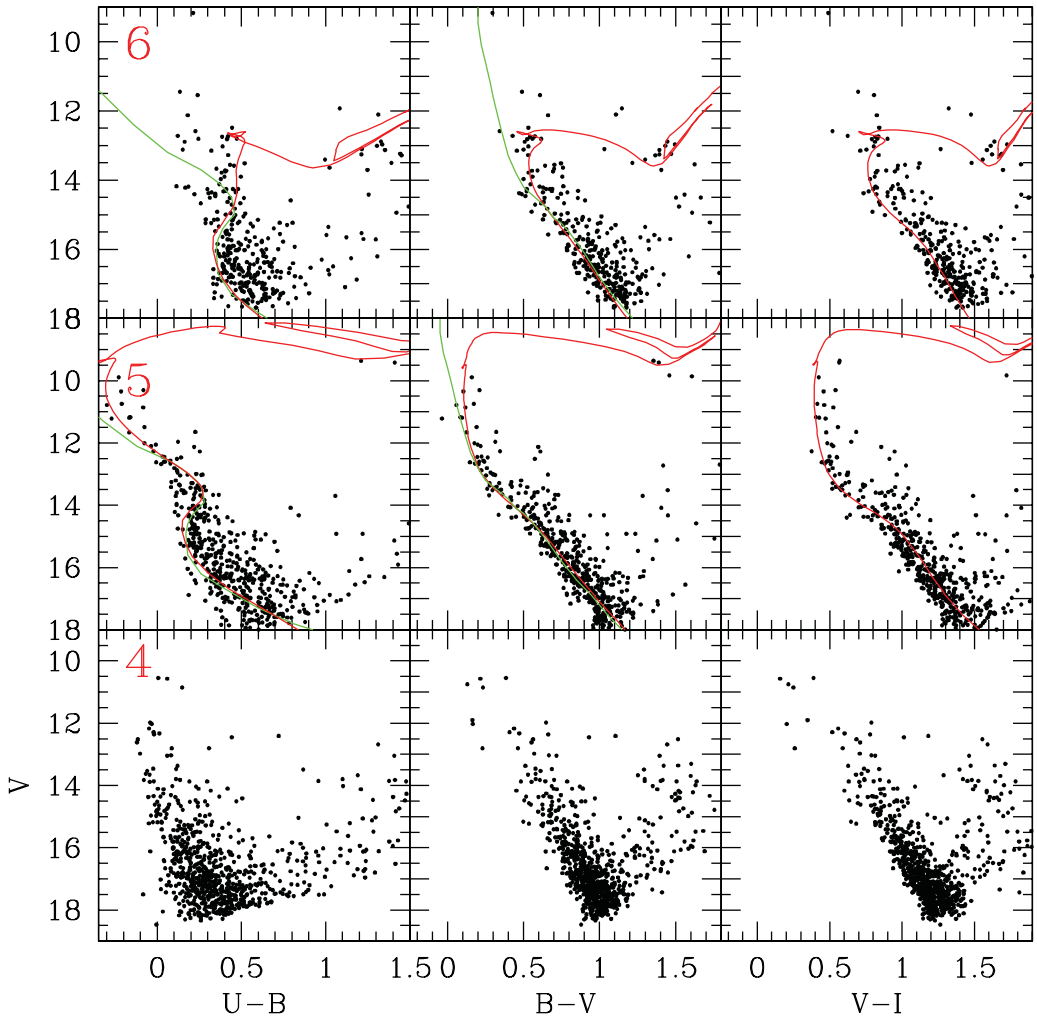

Figure 10. CMDs in the $V/U-B, V/B-V$ and $V/V-I$ for NGC 5284, NGC 5316 and NGC 5715. Numbering follows as in Table 1. The green line is an empirical ZAMS shifted by an amount corresponding to the apparent distance modulus to fit the cluster sequence. The red lines are isochrones from Marigo et al. (2008).

from the Sun and at 7.2 kpc from the Galactic Centre, beyond the Carina–Sagittarius arm. This location explains its significant reddening. Like NGC 5715, Czernik 38 is thus a Hyades-like cluster located in the inner disc, which managed to survive longer than the mean Galactic cluster lifetime.

8 CONCLUSIONS

We have presented and discussed *UBVI* photometry data for nine objects catalogued as Galactic clusters, for which only limited, if any, data were available. Structural parameters and fundamental properties have been derived and are summarized in Tables 5 and 8, respectively.

The basic goal of this work was first to assess the reality of these objects using star counts. Secondly, when an overdensity was detected, we looked at photometric diagrams to probe whether stars producing the overdensity would also exhibit distinctive features in the TCD and CMDs.

This allowed us to propose that VdB-Hagen 164 is most probably not a star cluster, since its stars do not either define a spatial concentration or show clear sequences in the photometric diagrams.

We arrived at quite the same conclusion for ESO 131SC09 and NGC 5284 whose stars, in spite of showing some spatial concentration, do not produce any distinctive feature in photometric diagrams. The appearance of a star cluster is generated by a group of bright stars, probably physically uncorrelated. They closely resemble the so-called open cluster remnants (Loden 1973; Carraro 2006; Pavani & Bica 2007), which, in the majority of the cases, are found to be random accumulations of stars along the line of sight.

The remaining targets are found to be genuine, physical star clusters. Their ages range from 100 to 600 Myr. However, only two of them (NGC 5715 and NGC 6268) are very young, and their distances are compatible with the location of the Carina–Sagittarius arm (Russeil 2003). We can conclude that they formed inside the arm and are bona fide tracers of the arm, since with such ages they could not travel much away from their birthplace.

Unfortunately, we fail to find any young cluster located beyond the Carina–Sagittarius arm in the present sample. This clearly reflects the difficulty to penetrate the arm and to see further away because of the high density of dust and gas, unless absorption holes allow us to detect more distant clusters (see e.g. Vázquez et al. 2005; Baume et al. 2009).

© 2011 The Authors, MNRAS **419,** 3608–3623
Monthly Notices of the Royal Astronomical Society © 2011 RAS

Downloaded from http://mnras.oxfordjournals.org/ at Ural Federal University on March 27, 2015

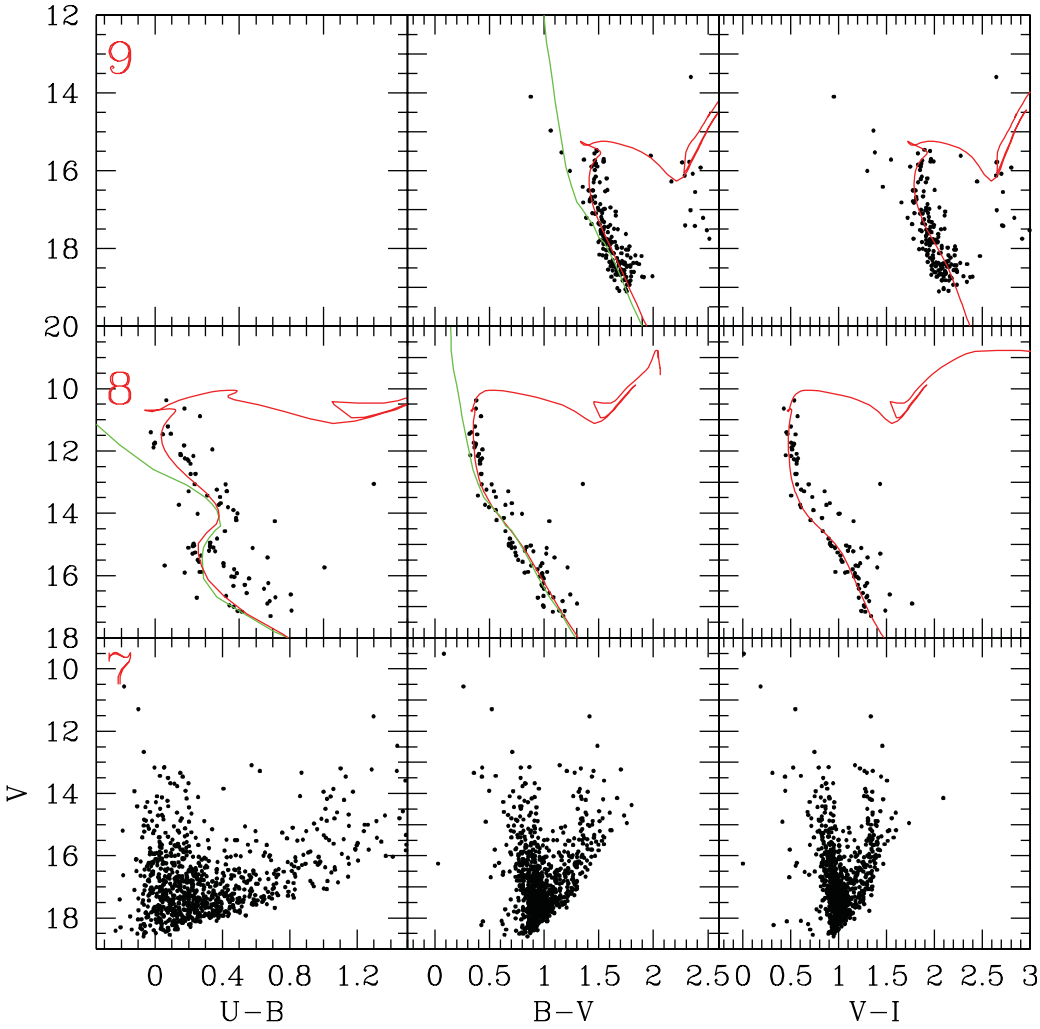

Figure 11. CMDs in the $V/U-B$, $V/B-V$ and $V/V-I$ for VdB-Hagen 164, NGC 6268 and Czernik 38. Numbering follows as in Table 1. The green line is an empirical ZAMS shifted by an amount corresponding to the apparent distance modulus to fit the cluster sequence. The red lines are isochrones from Marigo et al. (2008).

The oldest clusters (Czernik 38 and NGC 5715) are particularly interesting in the context of cluster dynamical evolution and dissolution models (Lamers et al. 2005), since they could survive longer than the typical open cluster in a dense and hostile environment such as the inner disc, where tidal forces and close encounters do not permit star clusters to survive typically more than 100–200 Myr (Wielen 1971).

Not many clusters of this age or older are known to be located at these Galactocentric distances (see e.g. http://www.univie.ac.at/webda/navigation.html). This combination of age and distance is extremely useful in investigating the Galactic disc radial abundance gradient in the inner disc (Magrini et al. 2010) and its evolution through time.

Therefore, these two clusters are ideal targets for a future spectroscopic follow-up to determine their metal abundances.

ACKNOWLEDGMENTS

We acknowledge the staff of CTIO and LCO, in particular Edgardo Cosgrove and Patricio Pinto, for their valuable support during the runs. AFS has been partly supported by the ESO Visiting Scientist Program. We are very grateful to Sandy Strunk, who carefully revised the paper and helped us to improve the language. This study made use of the SIMBAD and WEBDA data bases.

REFERENCES

Baume G., Carraro G., Momany Y., 2009, MNRAS, 398, 221
Becker W., 1960, Z. Astrophys., 51, 49
Bonatto C., Bica E., 2007, MNRAS, 377, 1301
Carraro G., 2006, Bull. Astron. Soc. India, 34, 153
Carraro G., Costa E., 2009, A&A, 493, 71
Carraro G., Méndez R. A., Costa E., 2005a, MNRAS, 356, 647
Carraro G., Dinescu D. I., Girard T. M., van Altena W. F., 2005b, A&A, 433, 143
Carraro G., Moitinho A., Vázquez R. A., 2008, MNRAS, 385, 1597
Carraro G., Vázquez R. A., Costa E., Perren G., Moitinho A., 2010, ApJ, 718, 683
Clariá J. J., Mermilliod J.-C., Piatti A. E., Minniti D., 1994, A&AS, 107, 39
Czernik M., 1966, Acta Astron., 16, 93
Dias W. S., Alessi B. S., Moitinho A., Lepine J. R. D., 2002, A&A, 389, 871
Dias W. S., Assafin M., Flório V., Alessi B. S., Líbero V., 2006, A&A, 446, 949
Dobbs C. L., Pringle J. E., 2010, MNRAS, 409, 396
Efremov Yu. N., 2011, Astron. Rep., 55, 108

Downloaded from http://mnras.oxfordjournals.org/ at Ural Federal University on March 27, 2015

Grosbol P., Carraro G., Beletski Yu., 2001, Messenger, 143, 47
Kharchenko N. V., Piskunov A. E., Röser S., Schilbach E., Scholz R.-D., 2005, A&A, 438, 1163
Lamers H. J. G. L. M., Gieles M., Bastian N., Baumgardt H., Kharchenko N. V., Portegies Zwart S. F., 2005, A&A, 441, 131
Landolt A. U., 1992, AJ, 104, 340
Lépine J. R. D., Roman-Lopes A., Abraham Z., Junqueira T. C., Mishurov Yu. N., 2011, MNRAS, 414, 1607
Loden L. O., 1973, A&AS, 10, 125
Maciejewski G., 2008, Acta Astron., 58, 389
Magrini L., Randich S., Zoccali M., Jilkova L., Carraro G., Galli D., Maiorca E., Busso M., 2010, A&A, 523, 11
Marigo P., Girardi L., Bressan A., Groenewegen M. A. T., Silva L., Granato G. L., 2008, A&A, 482, 883
Mermilliod J.-C., Mayor M., Udry S., 2008, A&A, 485, 303
Moitinho A., Vázquez R. A., Carraro G., Baume G., Lyra W., 2006, MNRAS, 368, L77
Moni Bidin C., de la Fuente Marcos R., de la Fuente Marcos C., Carraro G., 2010, A&A, 510, 44
Odenkirchen M., Soubiran C., 2002, A&A, 383, 163
Pancino E., Seleznev A. F., Ferraro F. R., Bellazzini M., Piotto G., 2003, MNRAS, 345, 683
Patat F., Carraro G., 2001, MNRAS, 325, 1591
Pavani D., Bica E., 2007, A&A, 468, 139
Platais I., Kozhurina-Platais V., van Leeuwen F., 1998, AJ, 116, 2423
Prisinzano E., Carraro G., Piotto G., Seleznev A. F., Stetson P. B., Saviane I., 2001, A&A, 369, 851
Ramin M. A., 1966, Astron. Nachr. 289, 41
Russeil D., 2003, A&A, 397, 133
Santos N. C., Lovis C., Pace G., Melendez J., Naef D., 2009, A&A, 493, 309
Schlegel D. J., Finkbeiner D. P., Dais M., 1998, ApJ, 500, 525
Schmidt-Kaler Th., 1982, in Schaifers K., Voigt H. H., eds, Landolt–Börnstein, Numerical Data and Functional Relationships in Science and Technology, New Series, Group VI, Vol. 2(b). Springer Verlag, Berlin, p. 14
Seggewiss W., 1968, Z. Astrophys., 18, 142
Seleznev A. F., Carraro G., Costa E., Loktin A. V., 2010, New Astron., 15, 61
Shaller G., Schaerer D., Meynet G., Maeder A., 1992, A&AS, 96, 269
Silverman B. W., 1986, Monographs on Statistics and Applied Probability. Chapman and Hall, London
Smiljanic R., Gauderon R., North P., Barbuy B., Charbonnel C., Mowlavi N., 2009, A&A, 502, 267
Stetson P. B., 1987, PASP, 99, 191
Trumpler R. J., 1930, PASP, 42, 214
Twarog B. A., Ashman K. M., Anthony-Twarog B. J., 1997, AJ, 114, 2556
van den Berg S., Hagen G. L., 1975, AJ, 80, 11
Vázquez R. A., Baume G., Feinstein C., Nunez J. A., Vergne M. M., 2005, A&A, 430, 471
Vázquez R. A., May J., Carraro G., Bronfman L., Moitinho A., Baume G., 2008, ApJ, 672, 930
Villanova S., Carraro G., de la Fuente Marcos R., Stagni R., 2004, A&A, 428, 67
Wielen R., 1971, A&A, 13, 309

This paper has been typeset from a TEX/LATEX file prepared by the author.

Downloaded from http://mnras.oxfordjournals.org/ at Ural Federal University on March 27, 2015